J Mol Model (2013) 19:3143–3151
DOI 10.1007/s00894-013-1848-2

ORIGINAL PAPER

# Computational insights into the binding modes of Sr-Rex with cofactor NADH/NAD$^+$ and operator DNA

**Yanyan Chu · Weihua Li · Jianfeng Wang · Guixia Liu · Yun Tang**

Received: 15 June 2012 / Accepted: 4 April 2013 / Published online: 25 April 2013


**Abstract** The transcriptional repressor Rex plays key roles in modulating respiratory gene expression. It senses the redox poise of the NAD(H) pool. Rex from *Streptomyces rimosus* (Sr-Rex) is a newly identified protein. Its structure and complex with substrates are not determined yet. In this study, the three-dimensional (3D) structural models of Sr-Rex dimer and its complex with cofactors were constructed by homology modeling. The stability of the constructed Sr-Rex models and the detailed interactions between Sr-Rex and cofactors were further investigated by molecular dynamics simulations. The results demonstrated that the conformation of Sr-Rex changed a lot when binding with the reduced NADH or oxidized NAD$^+$. Once binding with NADH, the Sr-Rex dimer displayed an opener conformation, which would weaken the interaction of Sr-Rex with Rex operator DNA (ROP). Key residues responsible for the binding were then identified. The computational results were consistent with experimental results, and hence provided insights into the molecular mechanism of Sr-Rex binding with ROP and NADH/NAD$^+$, which might be helpful for the development of biosensor.

**Keywords** DNA-binding protein · Homology modeling · Molecular dynamics · NADH/NAD$^+$ · Rex

## Introduction

Organisms have evolved their amount of enzymes to adjust their metabolisms. The transcription factor Rex is one of such enzymes that fine-tune metabolic fluxes during transition between aerobic and anaerobic environment [1]. Rex is a DNA-binding protein. Rex operator (ROP) sites are located upstream of several respiratory genes and ROP has been identified to be an 8-bp inverted repeat motif [2, 3]. Rex modulates respiratory gene expression by binding to NADH or NAD$^+$ in response to the changes of redox poise of the NADH/NAD$^+$ pool [3].

Rex generally functions as a homodimer. Each monomer contains two domains: the N-terminal domain contains a winged helix-turn-helix (HTH) DNA binding motif; and the C-terminal domain is a Rossmann fold domain, which contributes to pyridine nucleotide-binding. The two domains are connected by a flexible linker. The dimerization of *Thermus aquaticus* Rex (T-Rex) is primarily mediated by the C-terminal swapped α helices [4]. Till now, the crystal structures of Rex from *Thermus aquaticus* (PDB code: 1XCB [4], 3IKT [5], 3IKV [5], 3IL2 [5]), *Thermus thermophilus* HB8 (PDB code: 2DT5 [2]), *Bacillus subtilis* (PDB code: 2VT2 [6], 2VT3 [6]) and *Streptococcus agalactiae* (PDB code: 3KEO, 3KEQ, 3KET) have been determined and deposited in the Protein Data Bank (PDB).

In 2003, studies on Rex from *Streptomyces coelicolor* showed that NADH but not NAD$^+$ inhibits DNA binding, and NAD$^+$ competes with NADH for Rex binding, although both the reduced and oxidized forms of NAD(H) dinucleotide bind to Rex [3]. The same conclusion was also obtained in T-Rex studies because the addition of NADH can completely dissociate the T-Rex/DNA complex using surface plasmon resonance (SPR) assays [4]. Recently, studies on *Bacillus subtilis* Rex (B-Rex) found that B-Rex has a very high affinity for NADH, while its affinity for NAD$^+$ is 20,000 times lower.

Rex from *Streptomyces rimosus* (Sr-Rex) is a novel redox sensing repressor identified by our colleague Prof. Guo [7, 8]. They determined the sequence and reported that the

Y. Chu · W. Li · J. Wang · G. Liu · Y. Tang (✉)
Shanghai Key Laboratory of New Drug Design, School of Pharmacy, East China University of Science and Technology, 130 Meilong Road,
Shanghai 200237, China
e-mail: ytang234@ecust.edu.cn

binding of Sr-Rex with ROP could be adjusted by NADH in vitro [7, 8]. However, they could not understand the detailed molecular mechanism of Sr-Rex binding with ROP and/or NADH/$NAD^+$ from the observed experimental phenomenon. To solve this problem, at present work, we first constructed the 3D structural model of Sr-Rex by homology modeling. The interactions between Sr-Rex and cofactors as well as ROP were then explored by molecular dynamics (MD) simulations. From the computational results, which was consistent with the experimental reports [7, 8], we reasonably elucidated the molecular mechanism of Sr-Rex binding with its ROP and cofactor NADH/$NAD^+$, which might be very helpful for the development of biosensor.

## Methods

### Homology modeling of Sr-Rex

The primary sequence of Sr-Rex was provided by Prof. Guo, which was also available in the UniProt Knowledgebase (UniProtKB [9], entry code: C9EIM1 [10]). The blastp server was used to search the homologous proteins. Based on the sequence identity and resolutions, the crystal structure of T-Rex was chosen as the template and downloaded from PDB (PDB code: 3IKT [5]). The ROP coordinates and the water molecules were deleted from the crystal structure. The sequence alignment between the template and target was carried out by ClustalW 1.83 [11] using a gap penalty of 10 and PAM series weight matrix. The initial Sr-Rex models were then constructed by Modeller 9v8 [12] and the cofactor $NAD^+$ was retained in the corresponding position. The resulting models were validated by Procheck [13] and Profile-3D [14]. The best structural model was chosen for further modification and refinement.

Then, two copies of the best model was structurally aligned with the two monomers in the crystal structure of Rex from *Thermus thermophilus* (PDB code: 2DT5 [2]), separately. The formed homodimer Sr-Rex with cofactor was referred as oRex in the following. After removing $NAD^+$, the cofactor NADH was copied into the model from the crystal structure 2DT5, which was called rRex here after. The ROP sequence from T-Rex 5′-CGCTGTGAACGCGTTCACAGCG-3′ was used as the ROP of Sr-Rex. After the structures of oRex and rRex were built, the coordinate of ROP was merged to oRex and rRex from 3IKT, separately, which led to the corresponding models called oRex-ROP and rRex-ROP.

The constructed models were further prepared by adding all hydrogen atoms and charges with Protein Preparation Wizard in OPLS_2005 force field. The models were optimized by energy minimization in three steps using MacroModel [15], first minimizing hydrogen atoms only by constraining heavy atoms, then minimizing side chain with backbone constrained, finally relaxing the whole system. Both steepest descent and conjugate gradient methods were applied for energy minimization in each step. The resulted structures were used to run molecular dynamics.

### Molecular dynamics simulations

Sr-Rex has three histidine residues: His143, His214, and His225. Their protonation states were predicted by the PROPKA server (http://propka.ki.ku.dk/). According to the pka value from PROPKA, we set the residue type of His143 as HIE and His214 and His225 as HID.

Molecular dynamics simulations were performed on four systems, namely oRex, rRex, oRex-ROP, and rRex-ROP, separately. The all-atom model of each system was generated using xleap module in Amber10 [16] on the basis of the optimized model. Each system was then solvated with water in a truncated octahedron periodic box. The TIP3P water model [17] was used, and $Na^+$ counterions were added to neutralize the system. The distance between the box walls and the solute was set to 10 Å, so that the solute could not directly interact with its own periodic image given the cutoff in every system.

Prior to the production stage, two stages of energy minimization were performed to remove bad contacts. First, the solvent and counterions were relaxed by restraining the solute atomic positions with a harmonic potential. Second, all the atoms of the solute were relaxed without restraints. The two stages were both minimized by 500 steps of steepest decent minimization followed by 4500 steps of conjugate gradient minimization. After that, the system was gradually heated to 300 K over 30 ps using the NVT ensemble. In this procedure, the solute was restrained with a 10 kcal•$mol^{-1}$•$Å^{-2}$ harmonic force constant. And then the equilibration dynamics of the entire system was performed at 300 K for 100 ps [18, 19]. Finally, two 14 ns MD simulations for oRex and oRex-ROP and two 20 ns for rRex and rRex-ROP were conducted at 1 atm and 300 K with the NPT ensembles. During the simulation, SHAKE algorithm [20] was applied to constrain the covalent bonds to hydrogen atoms. A time step of 2 fs and a nonbond interaction cutoff radius of 10 Å were used. Coordinates were saved every 1 ps during the entire process. The ff03 all atom Amber force field [21] was used for the solute, and the force field parameters for the NAD(H) were adopted from Walker's calculation [22, 23].

## Results and discussion

### Homology modeling of Sr-Rex

#### *Construction of 3D models of Sr-Rex*

The first step to build a 3D model using homology modeling is to select a suitable template. A template structure search at

**Table 1** Homologous proteins of Sr-Rex

| PDB code | Source | Resolution (Å) | Cofactor | Identities (%) | Reference |
|---|---|---|---|---|---|
| 2DT5 | *Thermus thermophilus* | 2.16 | NADH | 45 | [2] |
| 3IKT | *Thermus aquaticus* | 2.26 | $NAD^+$ | 45 | [5] |
| 2VT3 | *Bacillus subtilis* | 2.00 | ATP | 39 | [6] |
| 3KEO | *Streptococcus agalactiae* | 1.50 | $NAD^+$ | 36 | |

the blastp server indicated that Sr-Rex has the highest sequence identity (~ 45 %) with the Rex family proteins from *Thermus thermophilus* (PDB code: 2DT5 [3] and 1XCB [4]) and *Thermus aquaticus* (T-Rex, PDB code: 3IKT [5], 3IKV [5] and 3IL2 [5]) (Table 1). Among these structures, 3IKT is the complex of Rex bound with $NAD^+$ and ROP, while 2DT5 and 1XCB are structures of Rex bound only with NADH. The RMS of monomers between 2DT5 and 3IKT is 1.9 Å, that is to say, the two monomers are very similar. To construct the complex of Sr-Rex bound with NAD(H) and ROP, the crystal structure 3IKT was chosen as the template.

The sequence alignment between Sr-Rex and T-Rex is illustrated in Fig. 1. Except for one gap inserted when sequence alignment, the majority of the structures were considered conserved. The resulting alignment was used as the input file for Modeller 9v8 to generate the initial 3D model of Sr-Rex homodimer.

The initial 3D model was submitted to energy minimization to release the bad atomic contact. Afterward, the minimized Sr-Rex model was assessed from the geometric aspect. The Procheck assessment results show that the 3D model has 92.2 % of residues located in the most favored regions, 6.4 % in the allowed regions, and 0.8 % in the generously allowed regions. The profile-3D evaluation shows that most of the residues have a score between 0 and 1 and only several residues have a score below 0. These assessments suggest that the constructed 3D model of Sr-Rex has reasonable quality relative to the crystal structures of T-Rex. The constructed model was used to build the starting structure for molecular dynamics.

*Construction of 3D models of Sr-Rex with cofactor and operator*

First, the NADH and $NAD^+$ cofactors were merged from 2DT5 and 3IKT to the constructed apo Sr-Rex model in turn. The complexes of Sr-Rex/NADH (rRex) and Sr-Rex/$NAD^+$ (oRex) were obtained. The ROP sequence of Sr-Rex is 5′-TGTGCACGCGTTCACA-3′ [7], while the corresponding sequence of T-Rex is 5′-TGTGAACGCGTTCACA-3′ [5]. The two sequences are quite similar. Based on the fact mentioned above and the modeled structures, ROP of the template was merged to rRex and oRex, finally rRex-ROP and oRex-ROP were built. By now, the four holo Sr-Rex models were constructed. The models of Sr-Rex bound to NADH, NADH/ROP, $NAD^+$, $NAD^+$/ROP were denoted as rRex, rRex-ROP, oRex, oRex-ROP, respectively, as shown in Fig. 2.

The built Sr-Rex structures were shown in Fig. 2, and the domain information was labeled in Fig. 2a. Similar to its homologues, Sr-Rex contains two domains: N-terminal domain (NTD) is a winged helix (WH) domain; and C-terminal domain (CTD) is a Rossmann folding domain. Sr-Rex forms homodimer by the C-terminal helix α8. The WH domains of Sr-Rex dimer show a V-shape conformation. The α3 helix of the WH domain positioned within the DNA major groove, and this conformation would stabilize the Sr-Rex binding with ROP.

## MD simulations of Sr-Rex complexes

To test the stability of our built 3D models of Sr-Rex and explore the dynamics behaviors of Sr-Rex in the different

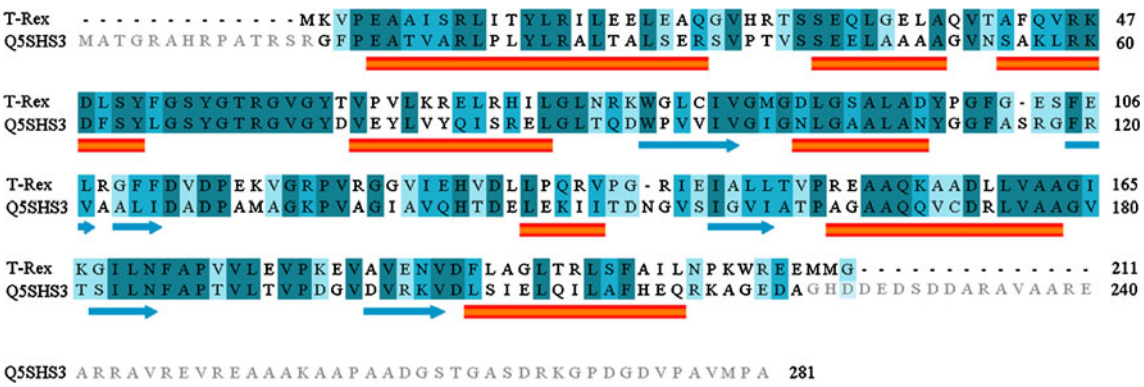


**Fig. 1** Sequence alignment between T-Rex and Sr-Rex (accession code: C9EIM1). The secondary structures were labeled under the sequence

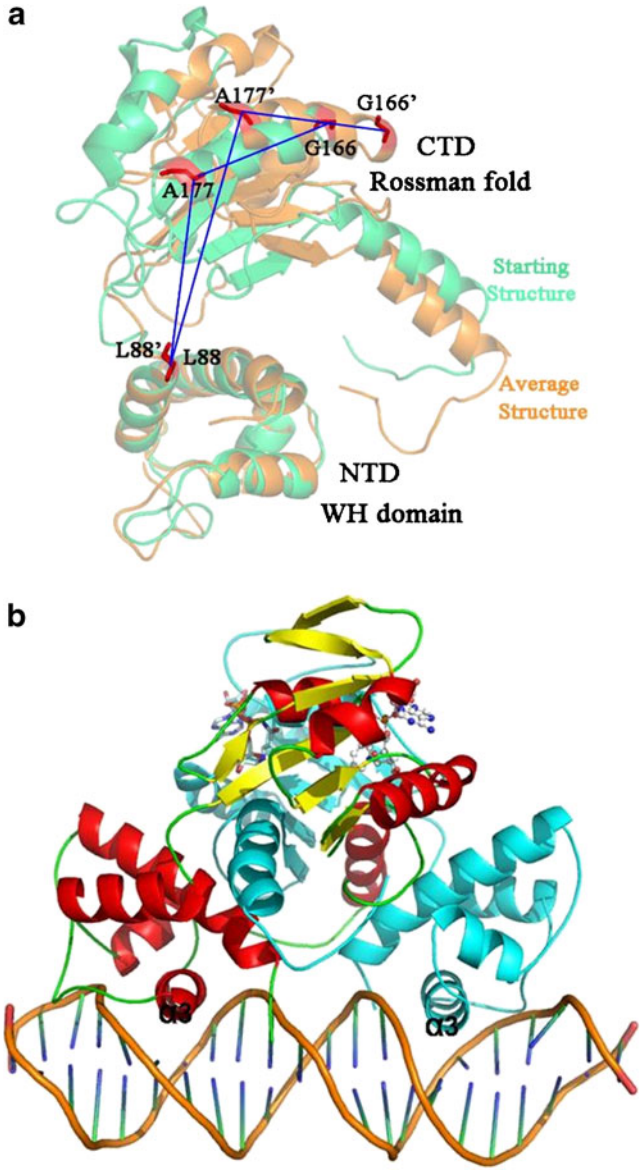


**Fig. 2** **a** Structure alignment between the average structure (*orange cartoon*) and the starting structure (*green cartoon*). Blue lines labeled the angles formed by Cα atoms from L88 through A177 to G166. The domain information was labeled. **b** Structures of Sr-Rex bound with NAD(H), with or without ROP binding. The reference position of ROP was shown

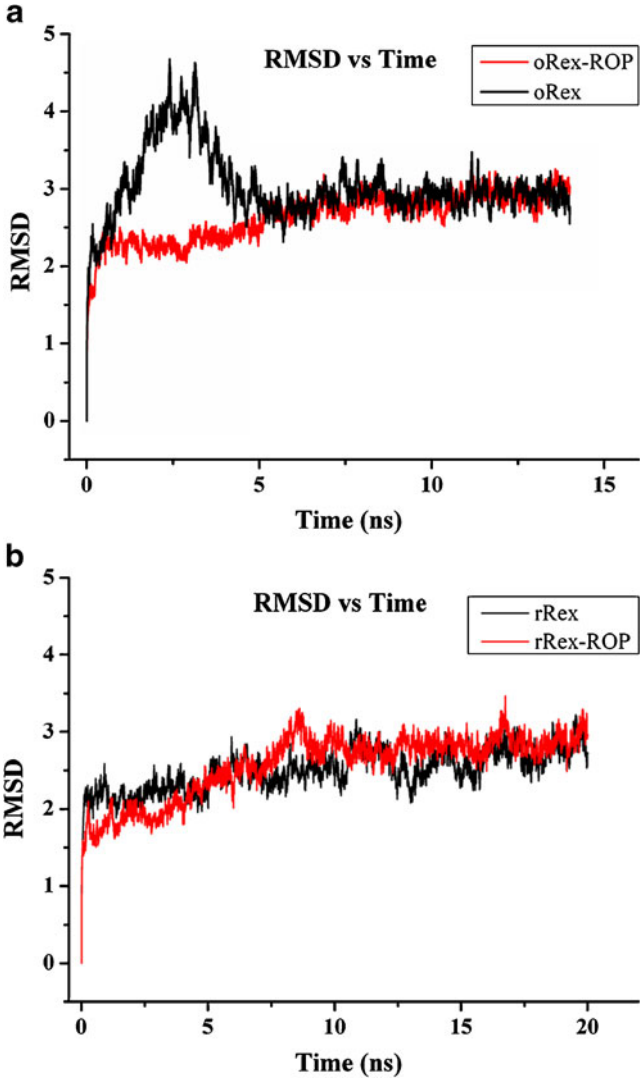


**Fig. 3** **a** Time dependence of the RMSD of oRex and oRex-ROP systems. **b** Time dependence of the RMSD of rRex and rRex-ROP systems

forms, MD simulations were performed on all four Sr-Rex systems.

*Overall structure changes*

The root-mean-square deviation (RMSD) values of protein backbone atoms with respect to the starting structures were monitored during MD simulations, as shown in Fig. 3. As seen from Fig. 3, the RMSD values of oRex and oRex-ROP systems reach stability after 6 ns, while the rRex and rRex-ROP systems take about 11 ns to reach a plateau. The relatively longer time to reach stability and larger fluctuation in RMSD also implied that the rRex and rRex-ROP systems have more flexibility than oRex and oRex-ROP.

To look into the mobility of the protein residues, the root-mean-square fluctuation (RMSF) of protein residues were calculated as shown in Fig. 4. By comparing the RMSF values of Sr-Rex with and without binding ROP, it is obvious that the fluctuations decreased after bound to ROP. Without binding to ROP, the value of the N-terminus of rRex can be up to ~3.0 Å, but the value decreased to 1.5 Å or lower when bound to ROP. This is also true for the oRex system.

*Conformational changes of Sr-Rex local sites*

Significant conformational differences were observed after MD simulations in the Sr-Rex local sites. Superimposition of the average structure of the last 2 ns MD simulations on the starting structures revealed that the Sr-Rex monomers

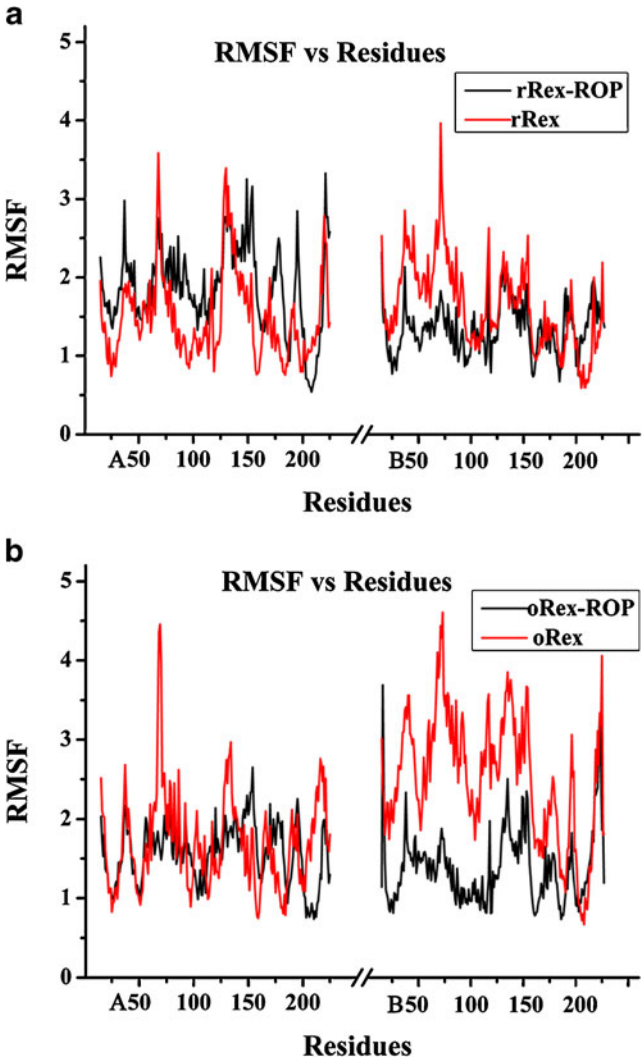


**Fig. 4** RMSF values of residues in different systems

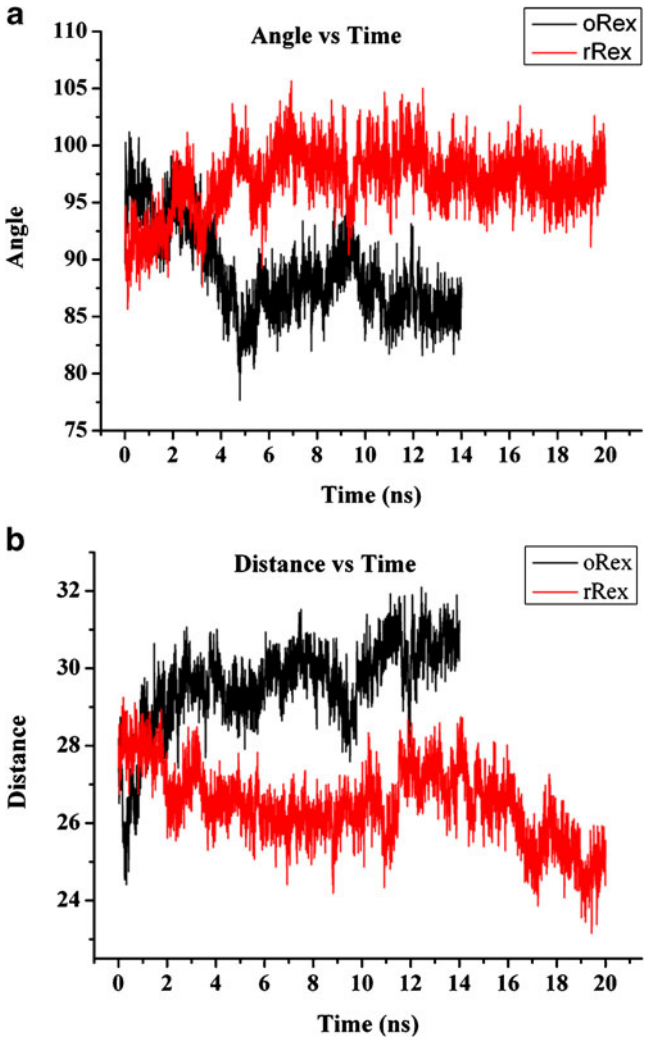


**Fig. 5** **a** Time dependence of the angle formed from L88 through A177 to G166 in oRex (shown in *black lines*) and rRex (labeled in *red lines*) systems. **b** Time dependence of the distance between Cα atom of L88 and that of A177 in oRex and rRex systems colored the corresponding colors

underwent a remarkable conformational change, which induced the change in dimers (Fig. 2a). The RMSD for all atoms is 2.9 Å, but the values become smaller for the individual domain, 1.2 Å for the WH domain and 1.5 Å for the Rossman domain. Therefore, the large conformational changes may ascribe to the loop region that links NTD and CTD. The loop is long and flexible, which is able to make the connected domains readily move. To confirm this idea, we identified the movement occurred between the two rigid domains. We defined an angle formed between the Cα atoms of L88, A177 and G166, to identify the twist of the two domains. The distance between the Cα atoms of L88 and A177 was used to identify the translation of the two domains. Figure 5a and b show the defined angle and distance vary with respect to simulation time. The angle in oRex expanded about 10° in clockwise rotation, whereas that in rRex increased about 10° in counter-clockwise rotation. Simultaneously, the two domains underwent translation, which was manifested by the distance variations. The CTD of oRex moved about 5 Å away from NTD, and thus elongating the whole protein. By contrast, the CTD domain of rRex approached NTD, thus shortening the protein. Coincidently, comparing the crystal structures of the Rex family, we found that both the Rossmann folding domain and the WH domain are quite conserved. And the major differences results from the long loop located between the two domains, which is especially remarkable when comparing the structure of T-Rex with that of B-Rex [6].

To compare the relative movement between the two Sr-Rex monomers when bound to $NAD^+$ or NADH, the final snapshot of MD simulation was superimposed on the starting structure, shown in Fig. 6. The movement of the two monomers is in opposite direction and the movement size in rRex is larger compared to oRex. Previous studies have indicated that

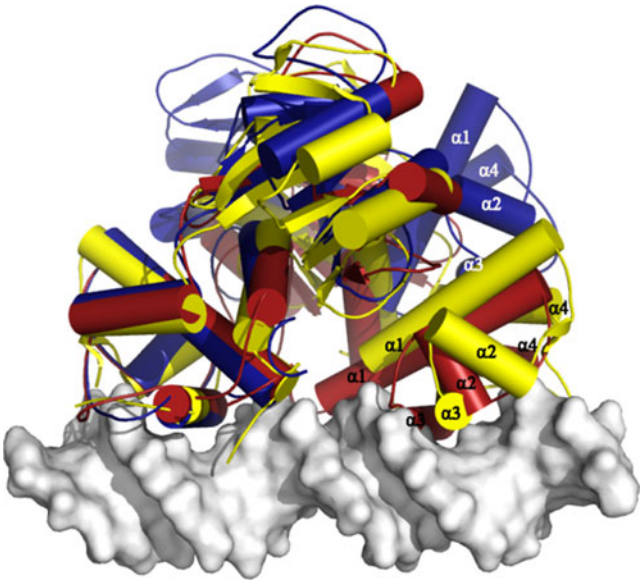


**Fig. 6** **a** Structure superimposition of Sr-Rex bound with NADH (*blue cartoon*) or $NAD^+$ (*red cartoon*) and 3IKT (*yellow cartoon*). ROP was located in the reference position by structure alignment and was shown in white surface

the two monomers exist in a closed form after T-Rex binds with NADH [6]. As such, it precludes T-Rex from binding to ROP. However, our results suggest Sr-Rex use a different mechanism from T-Rex. Based on our MD simulation results, we found that the two monomers in rRex could not maintain the initial open form, but became even more open after MD simulations, thereby loosing its contacts with ROP. We have analyzed the mean square displacement of all residues and found that the NTD domain had more movement when compared to CTD. Superimposition of the free ROP on the ROP in rRex revealed that one of the monomers did not have direct contact with ROP. This suggests that the binding of NADH to Sr-Rex led to the conformation of Sr-Rex to be more open, which is not favorable for ROP binding. This reminds us that the function mechanism that Sr-Rex dissociates from ROP when binding with NADH might be similar to B-Rex, whose homodimer shows an open conformation with the two N-terminal domains splayed out [6]. In such a conformation, Rex can not bind with ROP.

### *Interactions between Sr-Rex with NADH/$NAD^+$*

Previous studies showed that there was a significant difference between the binding affinities of Sr-Rex with $NAD^+$ and NADH [7]. Therefore, the detailed interactions between $NAD^+$ and NADH with Sr-Rex were analyzed (Fig. 7). The conformations of $NAD^+$/NADH binding pockets in the two complexes had little difference. Both $NAD^+$ and NADH formed hydrogen bonding with Asp126, Asn103 and Thr163. In addition, $NAD^+$ formed hydrogen bonding with Thr144, Leu104 and Tyr111'. Interestingly, a water molecule was located nearby $NAD^+$ (Fig. 7a). $NAD^+$ interacted with Gly100, Gly102, Gly105 and Ala162 with the assistance of the water bridge. To validate the importance of this water, the distances between the O atom of water and the O atom of Gly100, the N atom of Gly102 and Gly105, as well as $NAD^+$ O9 were calculated. Figure 7c shows that the distances decreased sharply in the first several hundred picoseconds. This implies that the water molecule enters the $NAD^+$ binding pocket from somewhere away from the binding site. Once entering the pocket, it was captured by its surrounding atoms. In contrast, no such water was observed in the Sr-Rex/NADH complex. Since there are no residues that form strong interactions with the phosphate group of NAD(H), the existence of the water molecule could enhance the binding of $NAD^+$ with the protein.

The nicotinamide ring of $NAD^+$ formed a π-π face-to-face interaction with the phenyl ring of Tyr111'. After $NAD^+$ is reduced to NADH, the aromatic property of the substance disappears, and thus the π-π interaction can not be formed. In the Sr-Rex/NADH complex, the nicotinamide group formed hydrogen bonding with Phe186, Asp203, and Ser205. These interactions made the NADH orientation pointing to the protein interior and further stabilizing the conformation. All above factors lead to the different binding modes of $NAD^+$ and NADH in the binding pocket.

The binding of ROP with Sr-Rex had little influence on the binding conformation of NAD(H), both of which kept the hydrogen bonding with Asp126 and Asn103 (Fig. 8). However, the inclusion of ROP led to disappearance of the water that was observed in the Sr-Rex/$NAD^+$ complex. The loss of the water molecule might cause the binding affinity of $NAD^+$ to decrease. In the Sr-Rex/NADH complex, the purine ring underwent a twist and made a hydrogen bond with Gln70. In addition, the O8 atom of NADH formed a hydrogen bond with Tyr111'. The binding of ROP made the two monomers of the Rossman domain more compact thus enhancing the binding of NADH with them.

### *Key residues for Sr-Rex binding with ROP*

To examine the Sr-Rex-ROP interactions and the essential residues for ROP binding, we calculated the binding energy of Sr-Rex-ROP and further decomposed on individual residue. Figure 9 displayed the important residues that contribute to the Sr-Rex-ROP binding. It is clear that the residues with most favorable contributions to the binding energy are the positively charged residues, such as Arg23, Arg71, and Lys57. Because the ROP surface has many negatively charged phosphate groups, the positively charged residues in the WH domain of Sr-Rex have favorable electrostatic interactions with them. The ΔG values are lower than −10 kcal•$mol^{-1}$ or less. Instead, the negatively charged residues such as Glu45, Glu46, Asp61, Asp76 and Glu78 have the electrostatic

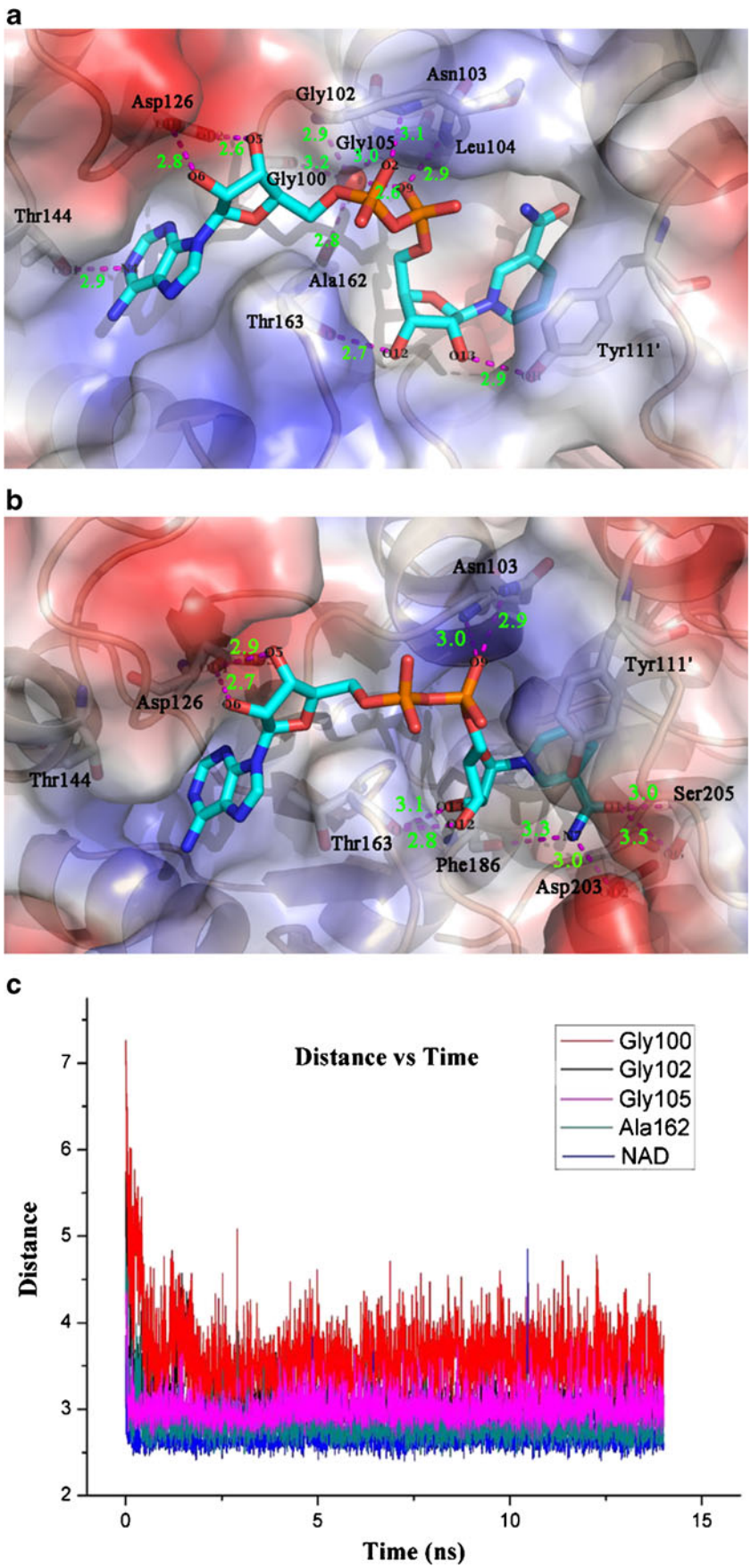


**Fig. 7** The binding mode of $NAD^+$ (**a**) or NADH (**b**) in Sr-Rex. Sr-Rex was shown in electrostatic surface, electropositive residues to electronegative residues colored from blue to red. The hydrogen bonds formed between Sr-Rex and $NAD^+$ or NADH were shown in dashed lines, and the lengths were labeled by the lines. The red sphere in Fig. 7a represented a water molecule. **c** Time dependence of the distances between O atom of the water molecule in Fig. 7a and O of Gly100, N of Gly102, N of Gly105, O of Ala162 or O9 of $NAD^+$

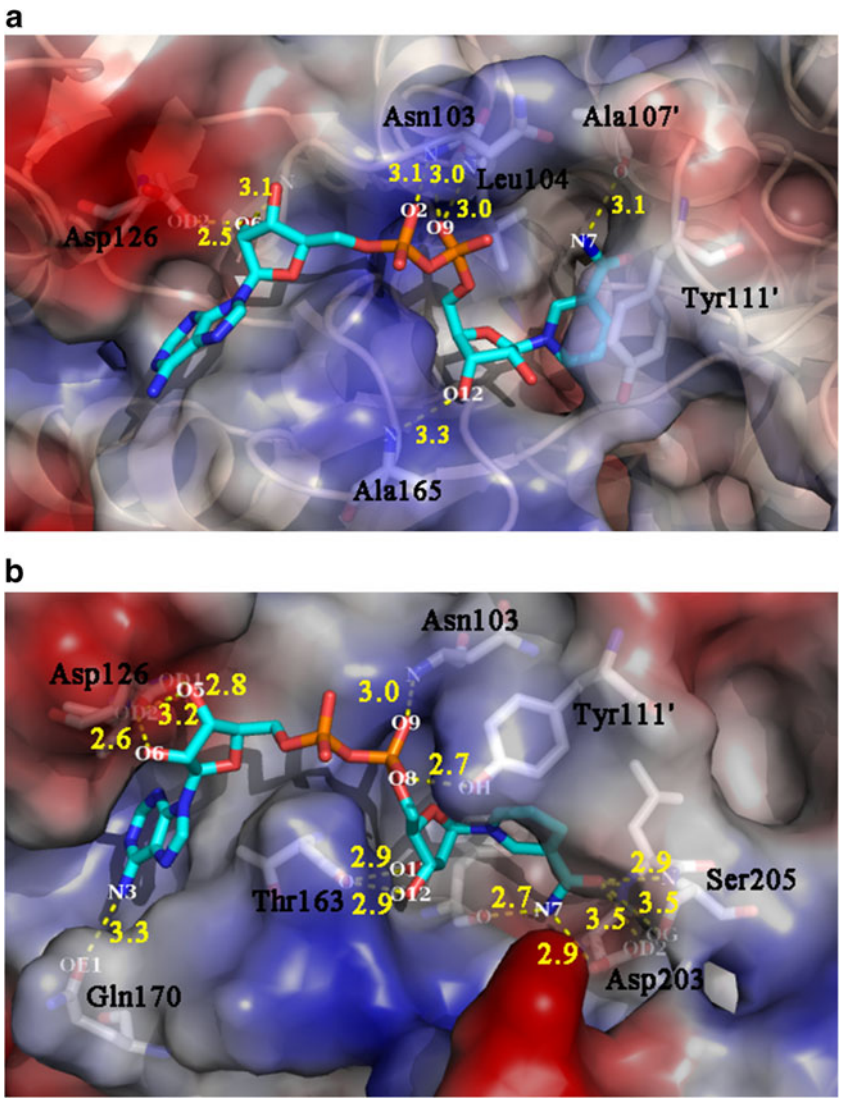


**Fig. 8** The binding mode of $NAD^+$ (**a**) or NADH (**b**) in Sr-Rex bound with ROP

repulsion with ROP and are unfavorable to ROP binding. The key residues that contribute greatly to the ROP binding in both monomers are almost identical. However, the free energies of certain residues such as Val59, Val73 and Glu18 have different contributions in both monomers. In addition to the electrostatic contribution, the van der Waals interactions between Pro17, Arg71, Gly72, Val73 also have contributions to the ROP binding.

## Conclusions

As a transcription factor, Rex plays essential roles in respiratory gene expression by sensing the poise of $NADH/NAD^+$, which rely heavily on the cellular redox stability. So Rex is essential in modulating cellular redox stability. Sr-Rex is a newly identified protein whose structure is unknown. To study the interaction of Sr-Rex with NAD(H) and ROP, we constructed the 3D models of Sr-Rex for the first time.

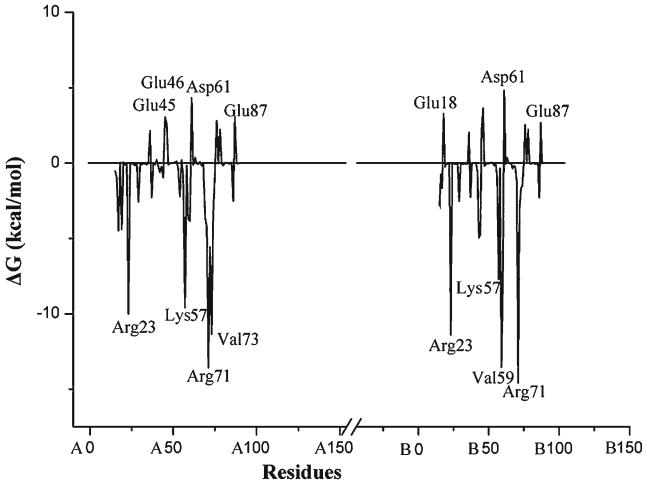


**Fig. 9** The contribution of the key residues to Sr-Rex and ROP binding

Validation from Procheck and Profile-3D showed that the constructed model was reasonable and reliable. Molecular dynamics simulations were then performed to study the interactions between Sr-Rex, NAD(H) and ROP. From the simulations, we found that the structures of the two domains, WH domain and Rossmann folding domain, composing the Sr-Rex monomer are conserved. There is long-range movement occurred between the two domains when Sr-Rex binds with NADH during the molecular dynamics simulations. The movement mainly results from the loop which is located between domains. Binding of NADH, Sr-Rex dimer presents a very open conformation with two WH domains splayed out, which made it incapable of binding with ROP. The results of the free energy decomposition showed that residues Arg23, Arg71, and Lys57 are essential for ROP binding. The findings will enhance our understanding of the function of Sr-Rex and provide some hints for the development of biosensor.

**Acknowledgments** The authors sincerely thank Prof. Meijin Guo for providing the primary sequence of Sr-Rex and helpful discussion. This work was supported by the Fundamental Research Funds for the Central Universities (Grant WY1113007) and the Shanghai Committee of Science and Technology (Grant 11DZ2260600).

## References

1. Weber W, Link N, Fussenegger M (2006) A genetic redox sensor for mammalian cells. Metab Eng 8(3):273–280
2. Nakamura A, Sosa A, Komori H, Kita A, Miki K (2007) Crystal structure of TTHA1657 (AT-rich DNA-binding protein; p25) from *Thermus thermophilus* HB8 at 2.16 Å resolution. Proteins 66(3):755–759
3. Brekasis D, Paget MS (2003) A novel sensor of NADH/NAD+redox poise in *Streptomyces coelicolor* A3(2). EMBO J 22(18):4856–4865
4. Sickmier EA, Brekasis D, Paranawithana S, Bonanno JB, Paget MS, Burley SK, Kielkopf CL (2005) X-ray structure of a Rex-family repressor/NADH complex insights into the mechanism of redox sensing. Structure 13(1):43–54
5. McLaughlin KJ, Strain-Damerell CM, Xie K, Brekasis D, Soares AS, Paget MS, Kielkopf CL (2010) Structural basis for NADH/NAD+redox sensing by a Rex family repressor. Mol Cell 38(4):563–575
6. Wang E, Bauer MC, Rogstam A, Linse S, Logan DT, von Wachenfeldt C (2008) Structure and functional properties of the *Bacillus subtilis* transcriptional repressor Rex. Mol Microbiol 69(2):466–478
7. Shen J, Tang ZY, Xiao CE, Guo MJ (2012) Cloning and expression of the redox-sensing transcriptional repressor Rex and in vitro DNA-binding assay of the Rex and rex operator in *Streptomyces rimosus* M4018. Acta Microbiologica Sinica 52(1):38–43
8. Tang ZY, Zhuang YP, Ju C, Zhang SL, Herron P, Hunter LS, Guo MJ (2011) A molecular Redox Sensor from *Streptomyces rimosus* M4018 for Escherichia coli. Afr J Microbiol Res 5(31):5682–5688
9. http://www.uniprot.org/
10. http://www.uniprot.org/uniprot/C9EIM1
11. Thompson JD, Gibson TJ, Plewniak F, Jeanmougin F, Higgins DG (1997) The CLUSTAL_X windows interface: Flexible strategies for multiple sequence alignment aided by quality analysis tools. Nucleic Acids Res 25(24):4876–4882
12. Sali A, Blundell TL (1993) Comparative protein modelling by satisfaction of spatial restraints. J Mol Biol 234(3):779–815
13. Laskowski R, Macarthur M, Moss D, Thornton J (1993) PROCHECK: A program to check the stereochemical quality of protein structures. J Appl Cryst 26:283–291
14. Gribskov M (1994) Profile analysis. Methods Mol Biol 25:247–266
15. Schrödinger LLC (2008)MacroModel, version 9.6, Schrödinger, LLC, New York, NY
16. Case DA, Cheatham TE 3rd, Darden T, Gohlke H, Luo R, Merz KM Jr, Onufriev A, Simmerling C, Wang B, Woods RJ (2005) The Amber biomolecular simulation programs. J Comput Chem 26(16):1668–1688
17. Jorgensen WL, Chandrasekhar J, Madura JD, Impey RW, Klein ML (1983) Comparison of simple potential functions for simulating liquid water. J Chem Phys 79:926–935
18. Li W, Tang Y, Liu H, Cheng J, Zhu W, Jiang H (2008) Probing ligand binding modes of human cytochrome P450 2 J2 by homology modeling, molecular dynamics simulation, and flexible molecular docking. Proteins 71(2):938–949
19. Zhao Y, Li W, Zeng J, Liu G, Tang Y (2008) Insights into the interactions between HIV-1 integrase and human LEDGF/p75 by molecular dynamics simulation and free energy calculation. Proteins 72(2):635–645
20. Ryckaert JP, Ciccotti G, Berendsen HJC (1977) Numerical integration of the cartesian equations of motion of a system with constraints: molecular dynamics of n-alkanes. J Comput Phys 23(3):327–341
21. Duan Y, Wu C, Chowdhury S, Lee MC, Xiong G, Zhang W, Yang R, Cieplak P, Luo R, Lee T, Caldwell J, Wang J, Kollman P (2003) A point-charge force field for molecular mechanics simulations of proteins based on condensed-phase quantum mechanical calculations. J Comput Chem 24(16):1999–2012
22. Walker RC, de Souza MM, Mercer IP, Gould IR, Klug DR (2002) Large and fast relaxations inside a protein: calculation and measurement of reorganization energies in alcohol dehydrogenase. J Phys Chem B 106:11658–11665
23. Pavelites JJ, Gao J, Bash PA, Mackerell AD (1997) A molecular mechanics force field for NAD+NADH, and the pyrophosphate groups of nucleotides. J Comput Chem 18(2):221–239